19th International Conference on
TRANSPORT AND SEDIMENTATION OF SOLID PARTICLES
24-27 September 2019, Cape Town, South Africa

CFD SIMULATION OF SHEAR SETTLING IN NON-NEWTONIAN FLOW

Cees van Rhee[1], Peter Dobbe[2]

[1]Faculty of Mechanical Engineering and Marine Technology/Faculty of Civil Engineering and Geosciences, Delft University of Technology, Mekelweg 2, Delft, 2628 CD, T: +31 15 278 3973, F: +3115 278 5602, E-mail: C.vanRhee@tudelft.nl; [2]Faculty of Mechanical Engineering and Marine Technology, Delft University of Technology, Mekelweg 2, Delft, E-mail:peter@dobbe.org

Settling of particles in non-Newtonian fluid is important in the field of mining and dredging. A Volume of fluid CFD code is adapted to simulate the settling of particles under shear. A rheological model is implemented that includes the influence of the sand concentration on the yield stress and plastic viscosity. The code is capable of simulating the shear settling behaviour of a mixture of fine and coarse grained particles.

KEY WORDS: Non-Newtonian flow, Shear Settling.

1. INTRODUCTION

The flow of mixtures of coarse solids in a non-Newtonian fluid occurs in many industrial applications, mining and dredging. The behaviour in both pipelines and disposal sites is important since it determines energy and water consumption as well as the strength development of disposal sites. In this study, it is investigated whether the open source CFD software OpenFOAM is capable of simulating these complex flows, and particularly a mixture of sand and a non-Newtonian mixture carrier fluid. In Van Rhee (2017) a CFD model based on the OpenFOAM solver icoFoam was presented. It was shown that the code was capable of simulating a mixture of fine and coarse grained particles. The mixture of fine grained particles and water formed the carrier fluid which was modelled as a Bingham Plastic fluid. In this carrier fluid coarse grained particles were transported and partially settled due to the so-called shear settling mechanism. A shortcoming of the icoFoam solver is, however, that it is not capable of simulating free surface flows. For a uniform free surface flow, a rigid lid approach can be used to overcome this limitation, but the mixture depth must be known beforehand in that case. It is clear that for the free surface flow on a disposal site a more sophisticated approach is needed compared to a rigid lid approach.

ISSN 0867-7964 ISBN 978-83-7717-323-7 DOI 10.30825/4.12-30.2019

2. GOVERNING EQUATIONS

2.1 MASS AND MOMENTUM

As mentioned in the Introduction a free surface flow should be simulated. A possible approach is the use of the Volume Of Fluid (VOF) method. In that case a scalar quantity determines whether a grid cell is occupied by a fluid (below the mixture surface) or by air (above the mixture surface). In OpenFOAM this quantity is denoted α, where $\alpha = 1$ when a grid cell is filled with a fluid and $\alpha = 0$ when the grid cell is filled with air. In cells where the fluid interface is present values of α between 0 and 1 are also possible. In this paper we will use an adapted form of the interFoam solver of OpenFOAM. This is a mixture model, so only one momentum equation is solved. The momentum equation reads:

$$\frac{\partial U}{\partial t} + \nabla.(UU) - \nabla.\frac{\mu}{\rho}\nabla U - g - \frac{F_s}{\rho} = -\frac{1}{\rho}\nabla p \qquad (1)$$

where, U is the flow velocity, p is the pressure, μ is the viscosity, g is the acceleration due to gravity, ρ is the density of the fluid and F_s is the surface tension (here not playing an important role). The continuity equation takes the form:

$$\nabla.U = 0 \qquad (2)$$

The density is the weighted densities of the different fluids (mixture ρ_m and air ρ_a).

$$\rho = \alpha\rho_m + (1-\alpha)\rho_a \qquad (3)$$

The viscosity μ is averaged in the same way between the viscosity of the mixture and air. The mixture viscosity is calculated using a Bingham Plastic model:

$$\mu = \tau_y + \mu_p\,\dot{\gamma} \qquad (4)$$

The density of the mixture depends on the density of the carrier fluid ρ_c and the sand volume concentration fraction c_s.

$$\rho_m = c_s\rho_s + (1-c_s)\rho_c \qquad (5)$$

The (volumetric) sand fraction influences both yield stress τ_y and plastic viscosity μ_p, following Talmon et al. (2016):

$$\mu_p = \mu_{p,c}e^{\beta\lambda}$$
$$\tau_y = \tau_{y,c}e^{\beta\lambda} \qquad (6)$$

where $\mu_{p,c}$ and $\tau_{y,c}$ are the rheological parameters of the carrier fluid alone, β is a constant (in this study a value of 0.27 is chosen) according to Talmon et al. (2016) and λ the linear concentration defined as:

$$\lambda = \frac{1}{\left(\frac{c_{max}}{c_s}\right)^{\frac{1}{3}} - 1} \tag{7}$$

where c_{max} is the maximum volumetric concentration of the sand fraction.
The sand fraction c_s is being transported by the fluid fraction using the drift flux approach:

$$\frac{\partial c_s}{\partial t} + \nabla.(U_s c_s) = 0 \tag{8}$$

where the sand particles have a velocity U_s which is simply calculated with

$$U_s = U + w_s \tag{9}$$

in which w_s is the particle settling velocity.

2.2 SETTLING VELOCITY

The settling velocity is calculated using Talmon and Huisman (2005):

$$w_s = (1 - c_s)\frac{1}{18}\frac{(\rho_s - \rho)gd^2}{\mu} \tag{10}$$

Due to the high value of the viscosity Stokes Law is used and hindered settling is according to Spelay (2007) and not according to Richardson and Zaky. Where the first term between brackets denotes the hindered settling effect and μ is the apparent viscosity without the effect of the sand fraction.

3. NUMERICAL IMPLEMENTATION

The interFoam solver of OpenFOAM is used as a basis for the new solver. In interFoam a non-Newtonian viscosity model already can be used. However, the available models do not include the influence of the sand fraction on rheology as indicated above. Therefore, a new Bingham Plastic model is included. Furthermore, the transport Eq. (8) is added to the solver.

4. VALIDATION

4.1 2D CHANNEL FLOW CARRIER FLUID

The first step is the validation of the solver for a Bingham Plastic fluid without a coarse fraction (hence carrier fluid alone). The simulation is carried out for parameters shown in Table 1.

Table 1

Input parameters for 2D channel flow simulation

Quantity	Symbol	Value
Discharge	**Q**	4 l/s
Inflow area	**A**	0.1 m x 0.1 m = 0.01 m^2
Inflow velocity	**U**	4 m/s
Slope	$\boldsymbol{\theta}$	2.86 deg
Density carrier fluid	$\boldsymbol{\rho_c}$	1249 kg/m^3
Yield stress	$\boldsymbol{\tau_{y,c}}$	10 Pa
Plastic viscosity	$\boldsymbol{\mu_p}$	0.2 Pa s

The solids volume fraction α can be graphically shown across the domain using ParaView. Figure 1 shows this variable for t = 2000 s. At the inflow section the velocity is uniform over depth, hence some distance is needed to establish a flow velocity distribution according to a Bingham Plastic fluid. For larger distances the flow depth and other parameters become constant.

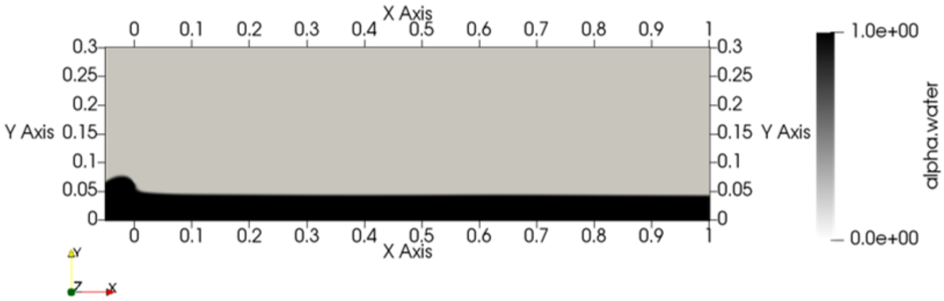

Figure 1. Value of the volume fraction α as a function of distance and depth

Figure 1 shows the volume fraction α. The figure shows a sharp interface between the fluid and the air above as expected therefore only two colors are visible for $\alpha = 0$ and $\alpha = 1$. The fluid enters the domain at the left side and flows into positive x-direction at x<0 and continues to flow in positive x-direction. The x-axis in the figure is distorted with a factor 20, hence the length of the horizontal axis is actually 20m.

The flow velocity distribution is compared with an analytical solution by De Kee et al. (1990).

for $h_p \leq y \leq h_0$

$$U_{x,shear} = \left(\frac{n}{n+1}\right)\left(\frac{K}{\rho g \sin\theta}\right)\left(\frac{\tau_b}{K}\right)^{\frac{n+1}{n}}\left(1-\frac{\tau_y}{\tau_b}\right)^{\frac{n+1}{n}}\left(1-\left(\frac{\frac{\tau}{\tau_y}-1}{\frac{\tau_b}{\tau_y}-1}\right)^{\frac{n+1}{n}}\right) \quad (11)$$

for $0 \leq y \leq h_p$

$$U_{x,plug} = \frac{nK}{(n+1)\rho g \sin\theta}\left(\frac{\tau_b}{K}\right)^{\frac{n+1}{n}}\left(1-\frac{\tau_y}{\tau_b}\right)^{\frac{n+1}{n}} \quad (12)$$

where y is height, h_p is the height of the plug, τ_b is the bed shear stress, θ is the slope of the channel and h_0 is the flow depth.

These equations are also valid for power law fluids. For a Bingham Plastic flow $n = 1$ and $K = \mu_p$. Figure 2 shows the flow velocity and shear stress distribution over depth. The agreement between the analytical solution U_x and the numerical simulation $U_{x,sim}$ is good. The length of the flow domain for this simulation was 30 m. The profile was taken in the middle section of the domain at x= 15 m.

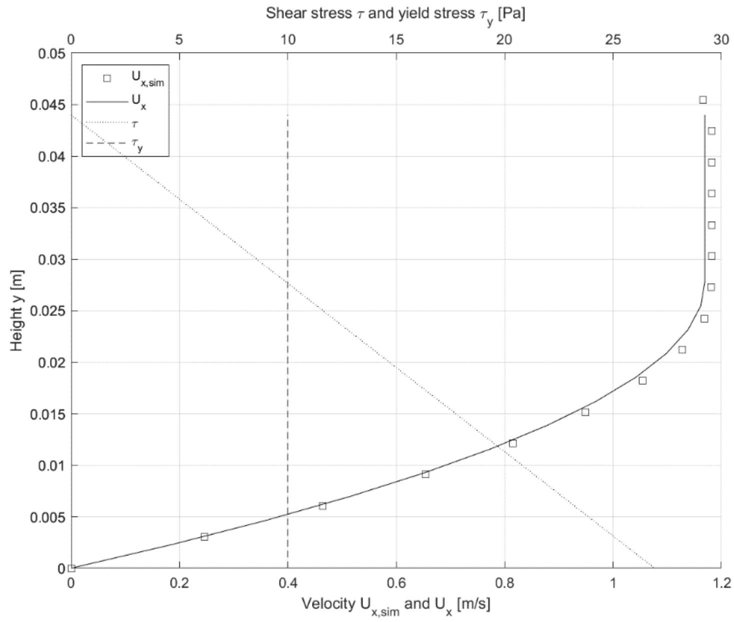

Figure 2. Calculated and analytical solution of the velocity distribution and shear stress distribution over depth at distance x = 15 m from the inlet zone

4.2 2D CHANNEL FLOW WITH SAND

The goal of this simulation is to see whether we can add a sand fraction to the Bingham Plastic modeled fluid and evaluate its flow properties. Next, we should see that sand is settling towards the bottom of channel. Further, we expect to see a lower sand concentration in the shearing layer than in the plug zone because the plug zone is where the yield stress is preventing shear and also preventing settling of the sand particles. Table 2 shows the input parameters used in the simulation.

Table 2

Input parameters for 2D channel flow simulation with sand

Quantity	Symbol	Value
Discharge	Q	4 l/s
Inflow area	A	0.1m x 0.1m = 0.01 m^2
Inflow velocity	U	4 m/s
Slope	θ	2.86 deg
Density carrier fluid	ρ_c	1249 kg/m3
Yield stress	$\tau_{y,c}$	47.3 Pa
Plastic viscosity	μ_p	0.2 Pa s
Coeff in eq. (6)	β	0.27
Particle size	d	188 micron

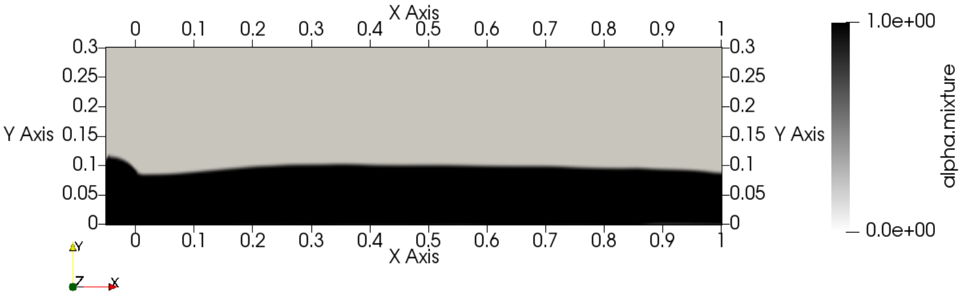

Figure 3. Value of the mixture volume fraction α as a function of distance and depth

Figure 3 shows the volume fraction as a function of height and distance for t = 600 s. Again, the fluid enters the domain from the left and flows in positive x- direction. The x-axis in the figure is distorted with a factor 20, hence the length of the horizontal axis is actually 20 m. The interface between the fluid and air remains sharp at this simulation. Similarly, the sand concentration can be shown. Figures 4 and 5 show this quantity at t = 600 s and t = 1200 s respectively.

The figures show that the sand particles remain in the fluid and are not entrained into the air fraction. This is logical since the viscosity of air is much lower compared with the viscosity of the fluid. So, when particles would be transported to the air-fraction they will immediately settle back into the fluid phase.

At the bottom of the fluid domain sand accumulates at a higher concentration as is also shown in Figure 6. The concentration reaches a maximum value of about 20% by volume. At this value the increased viscosity and yield stress will lead to a stagnation of the flow near the bed (see Figure 7). In the bed the shear rate will become zero leading to a high apparent viscosity and hence very low settling velocity of the coarse sand particles in this zone.

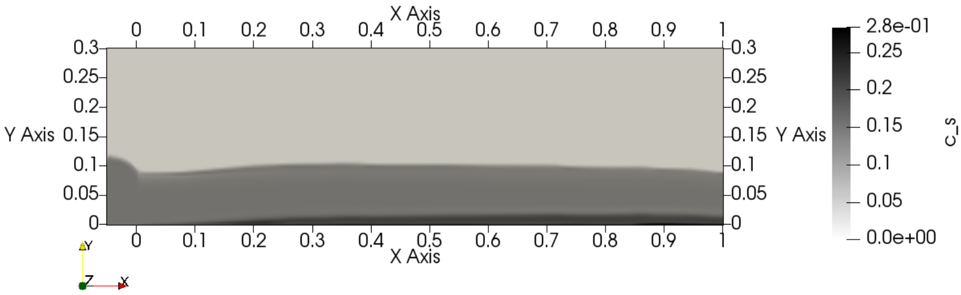

Figure 4. Calculated sand concentration fraction c_s at t = 600 s.

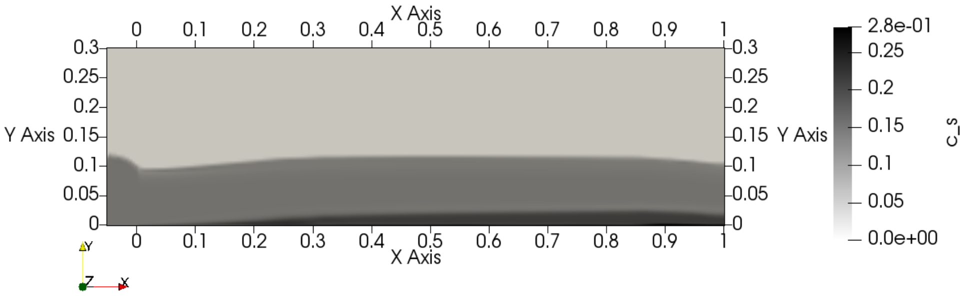

Figure 5. Calculated sand concentration fraction c_s at t = 1200 s.

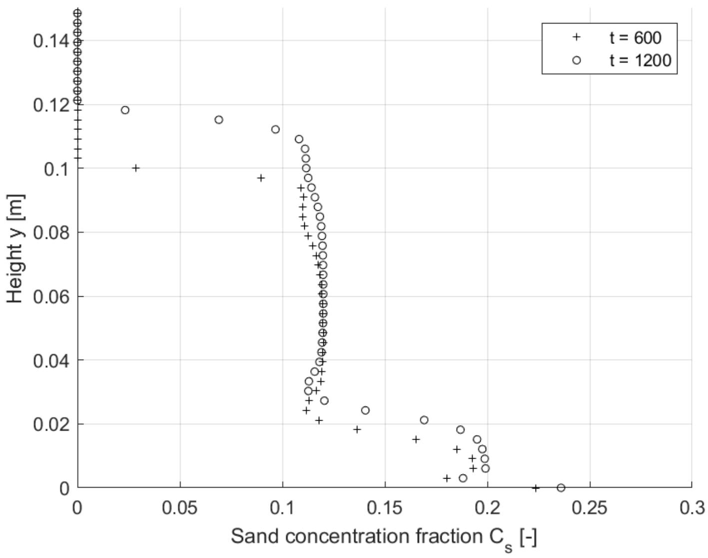

Figure 6. Calculated sand volume fraction c_s as a function of depth for t = 600 and t = 1200s

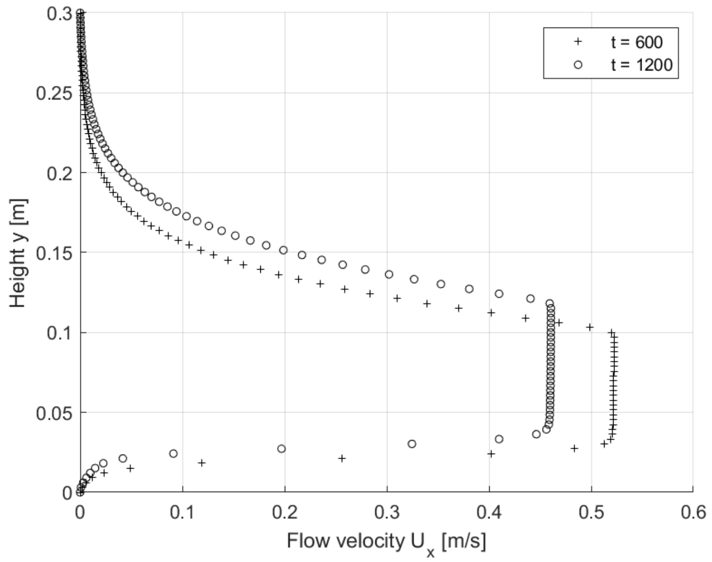

Figure 7. Flow velocity distribution U_x as a function of depth at x = 15 m and t = 600 and t = 1200s

The concentration near the bed shows a small dip. This is most probably caused by the bed boundary condition. This is subject to further study.

5. CONCLUSION

The adapted interFoam solver is capable of capturing the settling process of solid particles in a non-Newtonian free surface channel flow. The paper describes only a first attempt. In the future different settling models and rheological models will be tested. The model will also be used to simulate 3D pipe flow experiments.

REFERENCES

1. De Kee, D., Chhabra, R. P., Powley, M. B., & Roy, S., 1990. Flow of viscoplastic fluids on an inclined plane: evaluation of yield stress. Chemical Engineering Communications, 96, 1, 229-239. doi:https://doi.org/10.1080/00986449008911493
2. Talmon, A.M., Huisman, M, 2005, Fall velocity of particles in shear flow of drilling fluids, Tunnelling and Underground Space Technology 20, pp 193–201.
3. Talmon. A.M., Hanssen, J.L.J., Winterwerp, J.C. , Sittoni, L., Rhee, C. van, 2016, Implementation of Tailings Rheology in a Predictive Open-Channel Beaching Model, PASTE 2016, 19th International Seminar on Paste and Thickened Tailings.
4. Van Rhee, C., 2017, Simulation of the settling of solids in a non-Newtonian fluid, 18th Transport and Sedimentation Conference, Prague.